

ATMOSPHERIC REFRACTIVE ELECTROMAGNETIC WAVE BENDING AND PROPAGATION DELAY

JEFFREY G. MANGUM

National Radio Astronomy Observatory, 520 Edgemont Road, Charlottesville, VA 22903, USA

AND

PATRICK WALLACE

RAL Space, STFC Rutherford Appleton Laboratory, Harwell Oxford, Didcot, Oxfordshire, OX11 0QX, United Kingdom

Draft version March 30, 2015

ABSTRACT

In this tutorial we summarize the physics and mathematics behind refractive electromagnetic wave bending and delay. Refractive bending and delay through the Earth's atmosphere at both radio/millimetric and optical/IR wavelengths are discussed, but with most emphasis on the former, and with Atacama Large Millimeter Array (ALMA) applications in mind. As modern astronomical measurements often require sub-arcsecond position accuracy, care is required when selecting refractive bending and delay algorithms. For the spherically-uniform model atmospheres generally used for all refractive bending and delay algorithms, positional accuracies $\lesssim 1''$ are achievable when observing at zenith angles $\lesssim 75^\circ$. A number of computationally economical approximate methods for atmospheric refractive bending and delay calculation are presented, appropriate for astronomical observations under these conditions. For observations under more realistic atmospheric conditions, for zenith angles $\gtrsim 75^\circ$, or when higher positional accuracy is required, more rigorous refractive bending and delay algorithms must be employed. For accurate calculation of the refractive bending, we recommend the Auer & Standish (2000) method, using numerical integration to ray-trace through a two-layer model atmosphere, with an atmospheric model determination of the atmospheric refractivity. For the delay calculation we recommend numerical integration through a model atmosphere.

Subject headings: atmospheric effects, telescopes

1. INTRODUCTION

The path through the Earth's atmosphere of an electromagnetic wave emitted by an astronomical source deviates from a straight line connecting source and observer. This deviation is due to changes in the real portion of the refractive index of the Earth's atmosphere, defined as the ratio of the speed of light in a vacuum and the phase velocity in the medium through which the electromagnetic wave propagates:

$$n \equiv \frac{c}{v_{\text{phase}}}. \quad (1)$$

These changes in the refractive index of the atmosphere, combined with Fermat's principle, which states that an electromagnetic signal will follow the path between source and observer which takes the least amount of time, results in a path which is "curved". An observer on the surface of the Earth measures the effect of this curved path of the electromagnetic signal from the astronomical source as a deflection of the apparent position of the source and a delay in the arrival time of the electromagnetic signal. These two effects are generally referred to as atmospheric refractive electromagnetic wave bending and delay, respectively. Both of these effects lead to errors in astronomical position measurement. Atmospheric refractive bending leads to astronomical position errors measured by single telescopes, while atmospheric refractive delay leads to position errors measured by interferometers.

For refractive signal bending an observer measures

a difference between the unrefracted (or topocentric) zenith distance¹ of an astronomical source (z) and the observed zenith distance (z_0) of that source:

$$R \equiv z - z_0. \quad (2)$$

To relate this refractive signal bending to the refractive index n we introduce the "refractivity" at the observer (N_0), which is related to refractive index (n_0):

$$n_0 - 1 = 10^{-6}N_0, \quad (3)$$

where N_0 , measured in parts per million, is a function of the atmospheric pressure (P_0), temperature (T_0), and relative humidity (RH_0) at the observer.

The refractive delay experienced by an incoming electromagnetic wave due to its propagation through the Earth's atmosphere is given by:

$$\mathcal{L}_{\text{atm}} \equiv \int_s (n - 1) ds \quad (4)$$

where s is the path through and n is the refractive index of the atmosphere.

The goal of this tutorial is to provide a summary of the standard models used to calculate atmospheric electromagnetic signal bending and delay. With this summary we also discuss the limitations of these models and their relationship to example astronomical measurements. All of the refractive models we address are limited by the

¹ Astronomers use altitude, elevation (E) and zenith angle/distance (z) interchangeably. With but one exception, we have standardized the analyses presented in this tutorial by using zenith angle.

simplifications imposed by the parameterization of the Earth’s atmosphere (Section 3.1). For example, all of the atmospheric models we incorporate in our refractive signal analysis assume a static, homogeneous, two-layer (troposphere and stratosphere) atmosphere. We do not address, for example, effects due to time-variable atmospheric inhomogeneities (i.e. scintillation).

In this tutorial we begin by describing the physics of refractive bending (Section 2), which includes a discussion of the plane-parallel (Section 2.1) and radially-symmetric (Section 2.2) approximations to the calculation of refractive bending. We then review the general formalism used to describe refractive electromagnetic wave bending through the Earth’s atmosphere (Section 3), and describe a standard procedure used for calculating the refractive bending due to the Earth’s atmosphere. This discussion necessarily involves a model of the Earth’s atmosphere (Section 3.1). Our discussion of atmospheric refractive signal bending ends with a discussion of commonly-used approximations to the refractive bending (Section 3.2).

Our discussion of refractive delay (Section 4) describes the general formalism and common usage of “delay models”. This discussion of refractive delay includes an analysis of two additional corrections to the refractive delay at an antenna which is relevant to interferometric array observations: differential atmospheric curvature (Section 4.1.1) and antenna height correction (Section 4.1.2). Section 5 provides some background information on some of the generator function references presented, while Section 6 presents our conclusions. Throughout this tutorial application of the formalisms presented is made for the case of the propagation of radio through submillimeter wavelength electromagnetic radiation. We use the Atacama Large Millimeter Array (ALMA) as a source for many of these illustrative examples.

At a fundamental level the accuracy of the techniques presented in this tutorial are limited by the simplifications warranted by the need to model global atmospheric properties using local measurements. These simplifications include hydrostatic equilibrium for the dry component and uniform mixing of the wet component (mainly the troposphere) of the Earth’s atmosphere. Another major source of uncertainty is our limited understanding of the dispersive and non-dispersive refractive properties of the water molecule. We make no attempt to quantify these uncertainties rigorously, but do provide observational limits to the measured position of an astronomical source imposed by the simplified algorithms presented.

2. THE PHYSICS OF REFRACTIVE BENDING

As was noted in Section 1, the path of an electromagnetic wave through a refractive medium, such as the Earth’s atmosphere, is governed by Fermat’s Principle. Figure 1 displays the example of an electromagnetic signal propagating from one medium (i.e. vacuum) with index of refraction n_1 to another medium (i.e. the top of the Earth’s atmosphere) with index of refraction n_2 . Using the dimensions illustrated in Figure 1:

$$t = \frac{\sqrt{x_1^2 + y_1^2}}{v_1} + \frac{\sqrt{x_2^2 + y_2^2}}{v_2}, \quad (5)$$

where v_1 and v_2 are the phase velocities of the electromagnetic signal within each medium. Using the fact

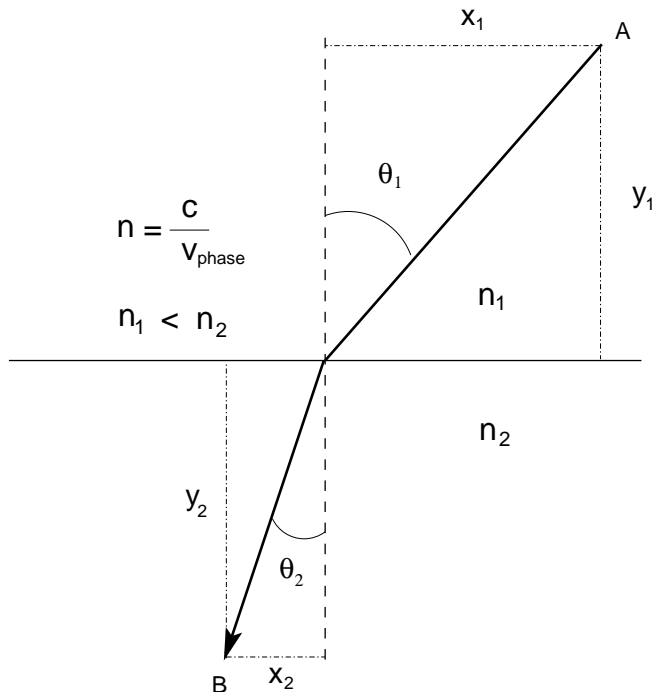


FIG. 1.— Diagram showing the propagation of an electromagnetic signal from one medium to another.

that the total vertical distance that the electromagnetic signal will travel is given by $d = y_1 + y_2$, we can substitute for y_2 in Equation 5 and differentiate with respect to y_1 in order to find the minimum time needed for the electromagnetic signal to travel from point A to point B:

$$\frac{dt}{dy_1} = \frac{y_1}{v_1 \sqrt{x_1^2 + y_1^2}} - \frac{(d - y_1)}{v_2 \sqrt{x_2^2 + (d - y_1)^2}}. \quad (6)$$

Setting Equation 6 equal to zero and noting that $\sin \theta_1 = y_1 / \sqrt{x_1^2 + y_1^2}$, $\sin \theta_2 = y_2 / \sqrt{x_2^2 + y_2^2}$, and $n = c/v$, we find that:

$$n_1 \sin \theta_1 = n_2 \sin \theta_2, \quad (7)$$

which is Snell’s Law.

If we now assume that the refractive medium is composed of stratified layers which are radially-symmetric about a common center, we can derive an equation which relates the total amount of electromagnetic signal refraction to the local atmospheric conditions at the point of observation. Before deriving the exact form for the refraction it is instructive first to derive the approximate form for the refraction assuming a plane-parallel atmosphere.

2.1. Plane-Parallel Atmosphere

In the following we derive the approximate form for electromagnetic signal refraction when the medium through which the signal is propagating is assumed to be plane-parallel. This derivation follows closely and attempts to summarize that presented in three of the standard references for this work: Smart (1962), Bean & Dutton (1966), and Green (1985). A visualization of a stratified plane-parallel atmosphere is shown in Figure 2. Consider an atmosphere with N horizontally-stratified layers with refractive indices n_N, n_{N-1}, \dots ,

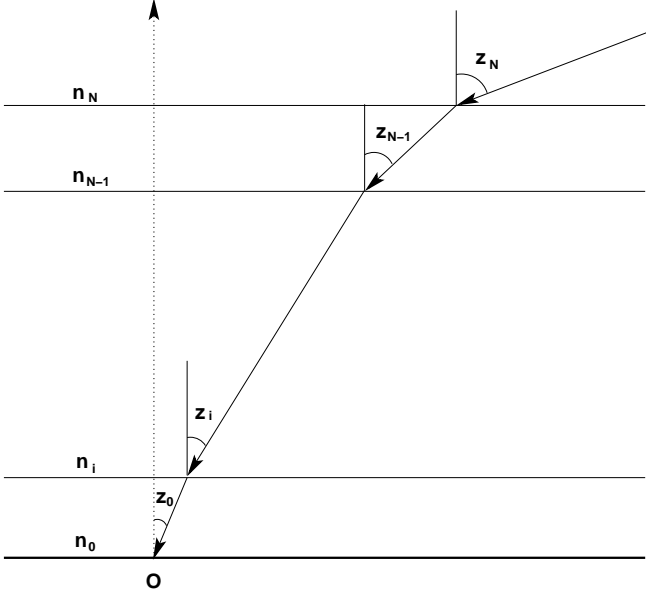


FIG. 2.— Diagram showing the propagation of an electromagnetic signal through a vertically-stratified atmosphere.

n_1 , n_0 . An electromagnetic signal entering the atmosphere at zenith angle z will be successively refracted through each layer, with the angle of refraction governed by Snell's Law (Equation 7):

$$n_i \sin z_i = n_{i-1} \sin z_{i-1}. \quad (8)$$

This successive application of Snell's Law results in the following relationship between the physical conditions at the top of the refractive medium and those at the point of observation:

$$\begin{aligned} n_0 \sin z_0 &= n_N \sin z_N \\ &= \sin z, \end{aligned} \quad (9)$$

where we have used the fact that the refractive index of free-space n_N is 1 and z_N is the unrefracted (or topocentric) zenith distance z . Defining the angle of refraction $R \equiv z - z_0$, and noting that $R \ll 1$, we can write Equation 9 as follows:

$$\begin{aligned} n_0 \sin z_0 &= \sin(R + z_0) \\ &= \sin R \cos z_0 + \cos R \sin z_0 \\ &\simeq R \cos z_0 + \sin z_0 \\ R &\simeq (n_0 - 1) \tan z_0 \text{ (radians)}. \end{aligned} \quad (10)$$

which is the equation for the total refraction in the limit of a stratified plane-parallel atmosphere. With the refractivity at the observer defined by Equation 3, the refraction at the observer, R_0 , is given by:

$$R_0 = 0.206265 N_0 (\text{ppm}) \tan z_o \text{ (arcsec)}. \quad (11)$$

Inserting the standard dry atmosphere value for $N_0 \simeq 280$ ppm yields:

$$R_0 \simeq 57.75 \tan z_0 \text{ (arcsec)}. \quad (12)$$

2.2. Radially-Symmetric Atmosphere

In the following we extend the formalism used to derive the refractive angle induced by a plane-parallel refractive medium to the general case of a radially-stratified atmosphere (Figure 3). As with our derivation of the

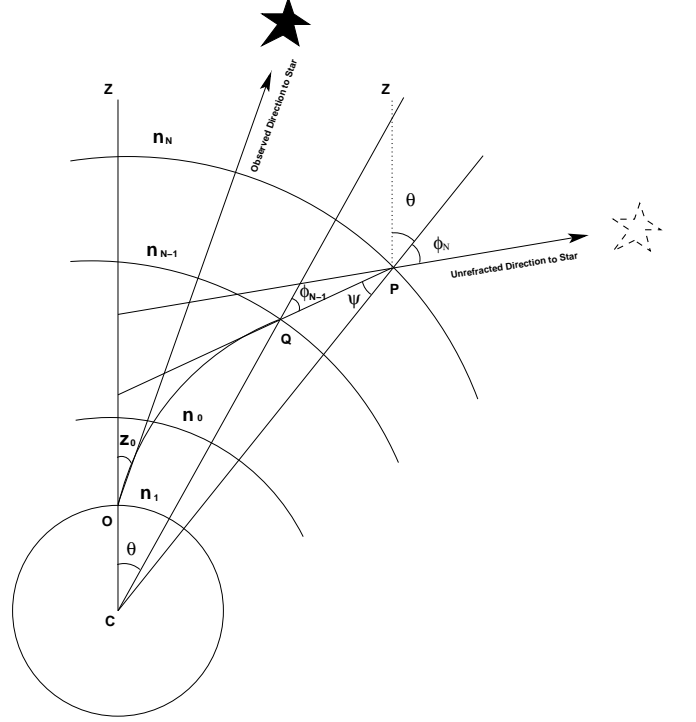


FIG. 3.— Diagram showing the propagation of an electromagnetic signal through a radially-stratified atmosphere.

refraction due to a plane-parallel medium, the following derivation follows closely and attempts to summarize that presented in three of the standard references for this work: Smart (1962), Bean & Dutton (1966), and Green (1985). We start with Snell's Law applied to the first layer of the atmosphere:

$$n_N \sin \phi_N = n_{N-1} \sin \psi, \quad (13)$$

and noting that, for the triangle CQP, with line segments $CP \equiv r_N$ and $CQ \equiv r_{N-1}$:

$$r_{N-1} \sin \phi_{N-1} = r_N \sin \psi. \quad (14)$$

Eliminating ψ from Equations 13 and 14:

$$n_N r_N \sin \phi_N = n_{N-1} r_{N-1} \sin \phi_{N-1}. \quad (15)$$

Applying Equation 15 to the last layer of the atmosphere above the observer:

$$nr \sin \phi = n_0 r_0 \sin z_0. \quad (16)$$

Noting that the unrefracted (topocentric) zenith angle z is given by:

$$z = \phi_N + \theta, \quad (17)$$

and that the angle ϕ_N is equal to the angle between r and the tangent to the angle θ :

$$\tan \phi_N = r_N \frac{d\theta}{dr}, \quad (18)$$

Since it is the variation of z with height above the observer that produces the total refraction at the observer, we need to take the differential of Equation 17 and use Equation 18:

$$\begin{aligned} dz &= d\phi_N + d\theta \\ &= d\phi_N + \frac{dr}{r_N} \tan \phi_N \end{aligned} \quad (19)$$

and Equation 16:

$$\begin{aligned} n_0 r_0 \sin z_0 &= (n + dn)(r + dr)(\sin \phi + d(\sin \phi)) \\ &= rn \sin \phi + rdn \sin \phi + ndr \sin \phi + rn \cos \phi d\phi \\ rn \cos \phi \left(d\phi + \frac{dr}{r} \tan \phi \right) &= -rdn \sin \phi, \end{aligned} \quad (20)$$

where we have kept only first-order terms in the differentials. Combining Equations 19 and 20:

$$dz = -\frac{dn}{n} \tan \phi, \quad (21)$$

after which we can integrate over all layers in the spherically-symmetric atmosphere, which results in the astronomical refraction, R , defined as the topocentric (i.e. unrefracted) zenith angle minus the observed (i.e. refracted) zenith angle:

$$R = \int_1^{n_0} \frac{\tan(z)}{n} dn \quad (22)$$

where n is the index of refraction, z is the zenith angle, and the integral is carried out along the path of the electromagnetic wave. In the next section we address the specific problem of calculating the refractive electromagnetic signal bending due to the Earth's atmosphere.

3. REFRACTIVE BENDING DUE TO THE EARTH'S ATMOSPHERE

Since the mid-1700s astronomers have studied refractive bending of electromagnetic waves due to the Earth's atmosphere in order better to understand the correspondence between measured and absolute positions of astronomical objects. Young (2004) presents a very thorough historical review of the development of our understanding of atmospheric refraction at optical wavelengths. The development of radio refraction algorithms parallels that described by Condon (2004) for the Green Bank Telescope. There have been many formulations of the equation which describes the bending of light through the Earth's atmosphere (see Young 2004). The following derivation of a generalized refractive bending calculation using a simple ray-trace analysis was originally proposed by Auer & Standish (1979)² and further developed by Hohenkerk & Sinclair (1985), and is described in Urban & Seidelmann (2013). A modern description of the algorithm can be found in Auer & Standish (2000). The *SLALIB*³ refraction function *slaRefro* uses a modified version of the Hohenkerk & Sinclair (1985) development of the Auer & Standish (1979) algorithm. Recent versions of *slaRefro* include an atmospheric model (Liebe et al. 1993) that allow for calculation of the atmospheric refractivity up to frequencies of 1 THz.

In principle, the refraction R could be calculated directly from Equation 22 by numerical quadrature. But, as Auer & Standish (1979, 2000) point out, numerical difficulties at $z = 90^\circ$ make it preferable to use z itself

² Although Young (2000) reports that the algorithm had in fact been derived and used by J. B. Biot in 1839.

³ *SLALIB* is the name of a widely used collection of positional-astronomy computer subprograms. A Fortran version released under the GNU General Public License is available from the Starlink Software Store: see <http://starlink.jach.hawaii.edu/starlink>. Proprietary C versions exist also.

as the variable of integration. Auer & Standish (2000) derive a transformed version of Equation 22 which varies slowly over z and avoids the numerical difficulties at $z = 90^\circ$. Following their derivation, Equation 22 can be written in terms of $\ln(n)$ as follows:

$$R = \int_0^{\ln(n_0)} \tan z d(\ln n). \quad (23)$$

Taking the logarithmic derivative of Equation 16

$$\begin{aligned} \ln(rn) &= \ln(n_0 r_0 \sin z_0) - \ln(\sin z) \\ \frac{d(\ln(rn))}{dz} &= -\frac{1}{\tan z} \end{aligned} \quad (24)$$

and substituting this expression into Equation 23

$$R = - \int_0^{\ln(n_0)} \frac{dz}{d(\ln(rn))} d(\ln n). \quad (25)$$

Further substituting the following

$$\begin{aligned} d(\ln(rn)) &= d(\ln r) + d(\ln n) \\ R(\ln n_0) &= R(z_0) \end{aligned} \quad (26)$$

leads to

$$\begin{aligned} R &= - \int_0^{z_0} \frac{d(\ln n)}{d(\ln r) + d(\ln n)} dz \\ &= - \int_0^{z_0} \frac{\frac{d(\ln n)}{d(\ln r)}}{1 + \frac{d(\ln n)}{d(\ln r)}} dz, \end{aligned} \quad (27)$$

which is Equation 3 from Auer & Standish (2000). Making the substitution

$$\frac{d(\ln n)}{d(\ln r)} = \frac{r}{n} \frac{dn}{dr} \quad (28)$$

leads to the following

$$R = - \int_0^{z_0} \frac{r \frac{dn}{dr}}{n + r \frac{dn}{dr}} dz. \quad (29)$$

Note that one can replace the refractive index n with the refractivity N using Equation 3.

Equation 29 is well-behaved at $z = 90^\circ$ and can be evaluated by quadrature using equal steps in z . At each step in z the corresponding values for r , n , and $\frac{dn}{dr}$ must also be calculated, thus requiring input from a model of the radial variation of P, T, and RH in the Earth's atmosphere (see Section 3.1). Values for r , n , and $\frac{dn}{dr}$ are found by finding the roots of Equation 16 as a function of r :

$$F(r) = nr - \frac{n_0 r_0 \sin z_0}{\sin z}. \quad (30)$$

One can find the root of Equation 30 by Newton-Raphson iteration, whereby the following equation is calculated with an initial guess (r_0) to find successive potential roots (r_1, r_2, \dots):

$$\begin{aligned} r_{i+1} &= r_i - \frac{F(r_i)}{F'(r_i)} \\ &= r_i - \left[\frac{n_i r_i - n_0 r_0 \frac{\sin z_0}{\sin z}}{n_i + r_i \frac{dn_i}{dr_i}} \right] \end{aligned} \quad (31)$$

for $i = 1, 2, \dots$, where r_i is the value of r calculated at the previous step of the integration, and we have used the fact that

$$F'(r) = \frac{dn}{dr}r + n. \quad (32)$$

Convergence of this iteration is fast, requiring only about 4 steps. Once one has a converged solution for r , n and $\frac{dn}{dr}$ can be calculated using the chosen atmospheric model.

The calculation then continues by integrating Equation 29 over each atmospheric interval (troposphere and stratosphere) using Simpson's rule with summation over equal steps in z

$$\int_{r_0}^{r_3} f(r)dr = \frac{\Delta r}{3} (f_0 + 4f_1 + 2f_2 + f_3), \quad (33)$$

where f_n is $f(x)$ evaluated at $x = x_0, x_1, x_2$, and x_3 . One can then compare each integration result with the result of the previous step of this integration. There is then a check for either convergence (*slaRefro* uses $|\int f(z_i)dz - \int f(z_{i-1})dz| \leq 10^{-8}$) or maximum iteration reached (*slaRefro* uses 16384). If convergence or maximum iteration has not been reached, recalculate r at each step in zenith distance by again solving Equation 29 using the procedure outlined above (Equation 31).

Equation 29 is the refraction equation used in Urban & Seidelmann (2013), Equation 7.80. A simple two component model of the atmosphere is often assumed. In this model, there is a discontinuity in $\frac{dn}{dr}$ at the tropopause, so the refraction integral must be calculated in two parts: one for the troposphere and another for the stratosphere. Note also that atmospheric inhomogeneities can be accounted for in this formalism by using multiple components in the integration.

3.1. Atmospheric Model

Equation 29 requires a description of the radial variation of n and its derivative $\frac{dn}{dr}$, which depend upon the radial variation of P , T , and RH in the Earth's atmosphere. A number of analytic expressions for $n(r)$ and $\frac{dn}{dr}$ have been used in the past, including the piecewise polytropic model of Garfinkel (1944, 1967). Following the atmospheric model described by Sinclair (1982) and Hohenkerk & Sinclair (1985), a simple two-component model for the Earth's atmosphere can be defined as follows:

- Spherically symmetric distribution of density with two layers (troposphere and stratosphere).
- Hydrostatic equilibrium.
- Perfect gas law applies.
- Temperature decreasing at a constant rate with height in the troposphere and constant in the stratosphere.
- The Gladstone-Dale relation, $n - 1 = a\rho$, which relates the refractive index n and the density ρ , where a is a constant which depends only on the local physical properties of the atmosphere.

- Two layer structure⁴ with $a < \infty$ for $r_e \leq r \leq h_t$ and $a = \infty$ for $h_t \leq r \leq h_s$.
- Constant relative humidity in the troposphere which is consequently equal to the relative humidity measured at the observer.
- The following constants:
 - Universal gas constant:
 $R_g = 8314.32 \text{ J}/(\text{mole} * \text{K})$
 - Molecular weight of dry air:
 $M_d = 28.9644 \text{ gm}/\text{mole}$
 - Molecular weight of wet air:
 $M_w = 18.0152 \text{ gm}/\text{mole}$
 - Molecular weight of atmosphere (mixture of dry and wet air): M_{atm}
 - Acceleration due to gravity at the center of mass of the vertical column of air above the observer at observer height h_0 : g_m . See Appendix B for further details on the preferred expression for g_m .
 - Height of the Earth's geoid (assuming WGS84 spheroid) as a function of latitude: $r_{WGS84} = 6378.137 \left(1 - \frac{\sin^2 \phi}{298.257223563}\right) \text{ km}$
 - Distance from the geoid to the observer: h_0
 - Distance from the geoid to the tropopause: h_t
 - Distance from the geoid to the limit of the stratosphere: h_s
 - Total height of the observer: $r_0 = r_{WGS84} + h_0$
 - Total height of the troposphere:
 $r_t = r_{WGS84} + h_t$
 - Total height of the stratosphere:
 $r_s = r_{WGS84} + h_s$

In the following we derive the radial variation of the temperature (T) and pressure (P).

3.1.1. Temperature Distribution

The distribution of temperature with r is defined as:

$$T(r) = T_0 + \alpha(r - r_0) \\ \frac{dT}{dr} = \alpha, \quad (34)$$

where α is often referred to as the "atmospheric temperature lapse rate". In the following analysis of the pressure distribution we will use these temperature relations.

3.1.2. Pressure Distribution

In the following we derive the distribution of pressure with height above the observer. The algorithm we describe follows closely that presented by Sinclair (1982), Murray (1983), and Hohenkerk & Sinclair (1985). Combining the ideal gas law:

$$P = \frac{\rho R_g T}{M_{atm}} \quad (35)$$

⁴ In the adopted atmospheric model the tropopause is a transition, not a layer.

and the equation for hydrostatic equilibrium:

$$\frac{dP}{dr} = -g_m \rho \quad (36)$$

and the temperature distribution relation (Equation 34) we find that:

$$\frac{dP}{P} = -\frac{g_m M_{atm}}{\alpha R_g} \frac{dT}{T}. \quad (37)$$

Integrating Equation 37 yields:

$$\begin{aligned} \int \frac{dP}{P} &= -\frac{g_m M_{atm}}{\alpha R_g} \int \frac{dT}{T} \\ \ln\left(\frac{P}{P_0}\right) &= \ln\left(\frac{T}{T_0}\right)^{-\frac{g_m M_{atm}}{\alpha R_g}} \\ \frac{P}{P_0} &= \left(\frac{T}{T_0}\right)^{-\frac{g_m M_{atm}}{\alpha R_g}} \\ &= \left(\frac{T}{T_0}\right)^\beta \end{aligned} \quad (38)$$

where we have defined:

$$\beta \equiv -\frac{g_m M_{atm}}{\alpha R_g}. \quad (39)$$

The total atmospheric pressure (P) and density (ρ) each have two components: the partial pressure and density due to dry air (P_d and ρ_d) and the partial pressure and density due to water (P_w and ρ_w). Since the water vapor pressure P_w decreases much more rapidly than the total pressure P , we need to separate P into its constituent parts. These pressures and densities are related as follows:

$$P = P_d + P_w \quad (40)$$

$$\rho = \rho_d + \rho_w \quad (41)$$

using the Ideal Gas Law (Equation 35) for each component (dry, wet, and total), we can write Equation 35 as:

$$\begin{aligned} P &= \frac{R_g T}{M_{atm}} (\rho_d + \rho_w) \\ &= \frac{P_d M_d + P_w M_w}{M_{atm}}, \end{aligned} \quad (42)$$

which allows us to write M_{atm} in terms of its dry and wet components as using Equation 40:

$$\begin{aligned} M_{atm} &= \frac{P_d M_d + P_w M_w}{P} \\ &= M_d - \frac{P_w (M_d - M_w)}{P}. \end{aligned} \quad (43)$$

Combining Equations 43, 37, and 38 produces a general expression which describes the variation of P with r :

$$\begin{aligned} \frac{dP}{P} &= \frac{-g_m M_d}{\alpha R_g} \frac{dT}{T} + \frac{g_m M_d P_w}{\alpha R_g P_0} \left(\frac{T}{T_0}\right)^{-\beta} \left(1 - \frac{M_w}{M_d}\right) \frac{dT}{T} \\ &= \beta \frac{dT}{T} - \beta \frac{P_w}{P_0} \left(\frac{T}{T_0}\right)^{-\beta} \left(1 - \frac{M_w}{M_d}\right) \frac{dT}{T}. \end{aligned} \quad (44)$$

Note that in Equation 44 g_m (Equation B8) and T (Equation 34) are known functions of r . Only the radial dependence of P_w is as yet unknown.

At this point we need to take a little diversion into the relationship between relative humidity (RH) and saturation vapor pressure (e_{sat}). In Appendix C we note that the approximation:

$$\frac{e_{sat}(P, T)}{e_{sat}(P_0, T_0)} = \left(\frac{T}{T_0}\right)^\gamma \quad (45)$$

for saturation vapor pressure agrees with the more exact expression (Equation C1: Buck (1981)) to within ± 0.2 hPa⁵ for P between 600 hPa and 1200 hPa and T between -30 C and $+20$ C. Therefore, using Equation 45 in Equation 44 yields:

$$\frac{dP}{P} = \beta \frac{dT}{T} - \beta \frac{P_w}{P_0} \left(\frac{T}{T_0}\right)^{\gamma-\beta} \left(1 - \frac{M_w}{M_d}\right) \frac{dT}{T}. \quad (46)$$

Integrating Equation 46 in the same way as for Equation 37 leads to the general expression which describes the radial dependence of atmospheric pressure:

$$\begin{aligned} \ln\left(\frac{P}{P_0}\right) &= \ln\left(\frac{T}{T_0}\right)^\beta + \frac{\beta}{\gamma-\beta} \left(1 - \frac{M_w}{M_d}\right) \\ &\quad \frac{P_w}{P_0} \left[1 - \left(\frac{T}{T_0}\right)^{\gamma-\beta}\right] \\ \frac{P}{P_0} &= \left(\frac{T}{T_0}\right)^\beta \exp(W) \end{aligned} \quad (47)$$

where we have defined:

$$W \equiv \frac{\beta}{\gamma-\beta} \left(1 - \frac{M_w}{M_d}\right) \frac{P_w}{P_0} \left[1 - \left(\frac{T}{T_0}\right)^{\gamma-\beta}\right]. \quad (48)$$

Sinclair (1982) points out that $W \lesssim 0.003$, which allows one to expand the exponential as $\exp(W) \simeq 1 + W$ and write Equation 47 as:

$$\begin{aligned} \frac{P}{P_0} &= \left(\frac{T}{T_0}\right)^\beta + \frac{\beta}{\gamma-\beta} \left(1 - \frac{M_w}{M_d}\right) \\ &\quad \frac{P_w}{P_0} \left[\left(\frac{T}{T_0}\right)^\beta - \left(\frac{T}{T_0}\right)^\gamma \right]. \end{aligned} \quad (49)$$

3.1.3. Application to the Troposphere and Stratosphere

In the following we list the parametric forms for $P(r)$, $T(r)$, $RH(r)$, n , and $\frac{dn}{dr}$ in the troposphere and the stratosphere:

⁵ Note that 1 hectopascal (hPa) = 1 millibar (mb) and that we use these two units interchangeably.

Troposphere:: ($r_e \leq r \leq h_t$)

$$T(r) = T_0 + \alpha(r - r_0) \quad (50)$$

$$P(r) = P_0 \left(\frac{T}{T_0} \right)^\beta + \frac{\beta P_{w0}}{\gamma - \beta} \left(1 - \frac{M_w}{M_d} \right) \left[\left(\frac{T}{T_0} \right)^\beta - \left(\frac{T}{T_0} \right)^\gamma \right] \quad (51)$$

$$RH(r) = RH_0 \text{ (constant)} \quad (52)$$

$$n = 1 + 10^{-6} N(r) \quad (53)$$

$$\frac{dn}{dr} = 10^{-6} \frac{dN(r)}{dr} \quad (54)$$

Stratosphere:: ($h_t \leq r \leq h_s$)

For isothermal atmospheric layers (like the stratosphere), $\alpha = 0$ and we use the approximation $\ln(1 + \epsilon) \rightarrow \epsilon$ as $\epsilon \rightarrow 0$, which makes Equations 34 and 38 become

$$T(r) = T(h_t) \text{ (constant)} \quad (55)$$

$$P(r) = P(h_t) \exp \left[-\frac{g_m M_{atm}(r - r_t)}{R_g T(h_t)} \right] \quad (56)$$

$$RH(r) = 0 \quad (57)$$

$$n = 1 + (n(h_t) - 1) \exp \left[-\frac{g_m M_{atm}(r - r_t)}{R_g T(h_t)} \right] \\ = 1 + 10^{-6} N(h_t) \exp \left[-\frac{g_m M_{atm}(r - r_t)}{R_g T(h_t)} \right] \quad (58)$$

$$\frac{dn}{dr} = -\frac{g_m M_{atm}(r - r_t)}{R_g T(h_t)} (n(r_t) - 1) \\ \exp \left[-\frac{g_m M_{atm}(r - r_t)}{R_g T(h_t)} \right] \\ = -\frac{g_m M_{atm}(r - r_t)}{R_g T(h_t)} 10^{-6} N(r_t) \\ \exp \left[-\frac{g_m M_{atm}(r - r_t)}{R_g T(h_t)} \right] \quad (59)$$

3.1.4. Atmospheric Radio/Submillimeter Refractivity

There are two ways to derive the atmospheric refractivity N_0 at the observatory for use in Equation 29:

1. Develop a closed-form expression for N_0^{rad} as functions of P and T .
2. Use an atmospheric model.

As the historical development of N_0 started with (1), which will also allow us to describe the physics behind this quantity, we revisit those expressions for $N_0 \equiv N_0^{rad}$ which are appropriate for calculations at radio and submillimeter wavelengths⁶.

In general, the refractivity of moist air at microwave frequencies depends upon the permanent and induced dipole moments of the molecular species that make up the atmosphere. The primary species that make up the

dry atmosphere, nitrogen and oxygen, do not have permanent dipole moments, so contribute to the refractivity via their induced dipole moments. Water vapor does have a permanent dipole moment. Permanent dipole moments contribute to the refractivity as $N_0^{rad} \propto \frac{P}{T^2}$, while induced dipole moments contribute as $N_0^{rad} \propto \frac{P}{T}$, where P is the pressure and T is the temperature of the species.

A simple parameterization of the frequency-independent (nondispersive) refractivity at the zenith is given by the Smith-Weintraub equation (Smith & Weintraub 1953):

$$N_0^{rad} = k_1 \frac{P_d}{T} + k_2 \frac{P_w}{T} + k_3 \frac{P_w}{T^2} + k_4 \frac{P_c}{T} \quad (60)$$

where P_d , P_w , and P_c are the partial pressures due to dry air, water vapor, and carbon dioxide, T is the temperature of the atmosphere, and k_1 , k_2 , k_3 , and k_4 are constants. The dry and wet air refractivities are then given by:

$$N_d = k_1 \frac{P_d}{T} \quad (61)$$

$$N_w = k_2 \frac{P_w}{T} + k_3 \frac{P_w}{T^2} \quad (62)$$

$$N_c = k_4 \frac{P_c}{T} = \frac{5}{3} \frac{P_c}{T}. \quad (63)$$

Since the partial pressure due to carbon dioxide is $\sim 0.04\%$ ⁷ of the total pressure, this term is often ignored or lumped into the dry air contribution in the simple parameterizations of atmospheric refractivity.

The dry air contribution to this refractivity (N_d) is primarily due to oxygen and nitrogen, and is nearly in hydrostatic equilibrium. Therefore, N_d does not depend upon the detailed behavior of dry air pressure and temperature along the path through the atmosphere, and can be derived based on local atmospheric temperature and pressure measurements. The wet air refractivity (N_w) can be inferred from local water vapor radiometry measurements.

Closed-form approximations for the nondispersive $N_0^{rad}(P, T)$ have been derived for use at frequencies below 100 GHz by Brussaard & Watson (1995):

$$^{BW} N_0^{rad} = 77.6 \frac{P_d}{T} + 72.0 \frac{P_w}{T} + 3.75 \times 10^5 \frac{P_w}{T^2} \text{ ppm} \\ = 77.6 \frac{P}{T} - 5.6 \frac{P_w}{T} + 3.75 \times 10^5 \frac{P_w}{T^2} \text{ ppm} \quad (64)$$

and Smith & Weintraub (1953) (see also Crane (1976) and Liebe & Hopponen (1977)):

$$^{SW} N_0^{rad} = 77.6 \frac{P_d}{T} + 72.0 \frac{P_w}{T} + 3.776 \times 10^5 \frac{P_w}{T^2} \text{ ppm} \\ = 77.6 \frac{P}{T} - 12.8 \frac{P_w}{T} + 3.776 \times 10^5 \frac{P_w}{T^2} \text{ ppm} \quad (65)$$

where

P_d is the partial pressure of dry gases in the atmosphere (in hPa),

⁶ For a brief description of atmospheric refractivity at optical wavelengths, see Appendix A

⁷ At present, this compares with less than 0.03% in pre-industrial times, and is currently increasing by more than 0.002% per decade.

P_w is the partial pressure of water vapor (in hPa),

P is the total barometric pressure (in hPa), which is equal to $P_d + P_w$, and

T is the ambient air temperature (in Kelvin).

The best of the closed-form approximations to the nondispersive refractivity, though, is the equation derived by R ueger (2002) which uses what he describes as the ‘‘best average’’ values for the coefficients k_1 , k_2 , and k_3 (which includes a 375 ppm contribution due to carbon dioxide in the k_1 term):

$$\begin{aligned} R_{ueger} N_0^{rad} &= 77.6890 \frac{P_d}{T} + 71.2952 \frac{P_w}{T} \\ &\quad + 3.75463 \times 10^5 \frac{P_w}{T^2} \text{ ppm} \\ &= 77.6890 \frac{P}{T} - 6.3938 \frac{P_w}{T} \\ &\quad + 3.75463 \times 10^5 \frac{P_w}{T^2} \text{ ppm}. \end{aligned} \quad (66)$$

Comparing these three closed-form expressions for radio refractivity at representative values of pressure, temperature, and relative humidity appropriate for the best ($P = 560$ hPa, $T = -20$ C, $RH = 0\%$) and worst ($P = 548$ hPa, $T = +20$ C, $RH = 100\%$) atmospheric conditions at the ALMA site (altitude = 5.0587 km) to a more exact model of the atmospheric refractivity (which includes a dispersive contribution), we find that:

- The Brussaard & Watson (1995), Smith & Weintraub (1953), and R ueger (2002) expressions agree to better than 0.1% for all conditions.
- The Brussaard & Watson (1995), Smith & Weintraub (1953), and R ueger (2002) expressions agree with a more exact (i.e. including dispersive refractivity; Liebe (1989)) atmospheric model prediction of N_0^{rad} to better than (see Figure 4):
 - Under the best ALMA atmospheric conditions:
 - * 0.08% at 8 GHz
 - * 0.13% at 230 GHz
 - * 0.13% at 370 GHz (this is a band edge for ALMA)
 - * 0.13% at 950 GHz (the highest band edge for ALMA)
 - Under the worst ALMA atmospheric conditions:
 - * 0.11% at 8 GHz
 - * 0.76% at 230 GHz
 - * 3.85% at 370 GHz
 - * 6.42% at 950 GHz

It is clear from this comparison that the closed-form expressions for N_0 are very good for calculations at frequencies far from telluric lines and for relatively dry conditions. For general high-accuracy calculations at sub-millimeter wavelengths which require better than 5% accuracy one should use an atmospheric model (such as

Liebe 1989; Liebe et al. 1993; Pardo et al. 2001) which incorporates both nondispersive and dispersive contributions to the refractivity to derive the total atmospheric refractivity.

3.2. Approximations to the Astronomical Refraction

Instead of using the integral Equation 22, various approximations are often made to reduce this expression to a simple analytic form. Some of the more generally useful forms are based on a generator function formalism which assumes an exponential atmospheric profile

$$N(h) = N_0 \exp \left[-\frac{(r - r_0)}{H} \right], \quad (67)$$

where r and r_0 are height coordinates and H is the effective height of the atmosphere

$$H = \frac{R_g T}{M_{atm} g_m}, \quad (68)$$

where R_g is the universal gas constant, M_{atm} is the molar mass of the atmosphere, T is the temperature of the atmosphere, and g_m is the gravitational acceleration constant measured at the center of the vertical column of air (see Section 3.1).

One form of this generator function formalism has been described by Yan & Ping (1995) and Yan (1996) as follows:

$$R_{generator} = R_0 m'(z) \sin z, \quad (69)$$

where R_0 is defined in terms of N_0 in Equation 11 and where the generator function $m'(z)$ is defined as follows:

$$m'(z) = \frac{1}{\cos z + \frac{A_1}{I^2 \sec z + \frac{A_2}{\cos z + \frac{13.24969}{I^2 \sec z + 173.4233}}}} \quad (70)$$

with

$$I = \sqrt{\frac{r_0}{2H}} \cot z. \quad (71)$$

See Mangum (2001) for further information on the use of this formalism for calculating the refraction. Note, though, that the analysis presented in Yan & Ping (1995) purports to achieve an accuracy far better than is realistic. Furthermore, comparisons with the refraction function *slaRefro* suggests that the parametric equation presented in Yan & Ping (1995) is tuned to a specific set of site and meteorological conditions (sea level and relatively dry).

An even simpler, though less exact, approximation to Equation 22 can be derived if one assumes a single-layer uniform atmosphere. Noting that Snell’s Law (Equation 7) reformulated in terms of zenith angle for a single-layer atmosphere (Equation 16 with $\phi = z$) becomes:

$$nr \sin z = n_0 r_0 \sin z_0, \quad (72)$$

we can solve for $\sin z$ and substitute into the trigonomet-

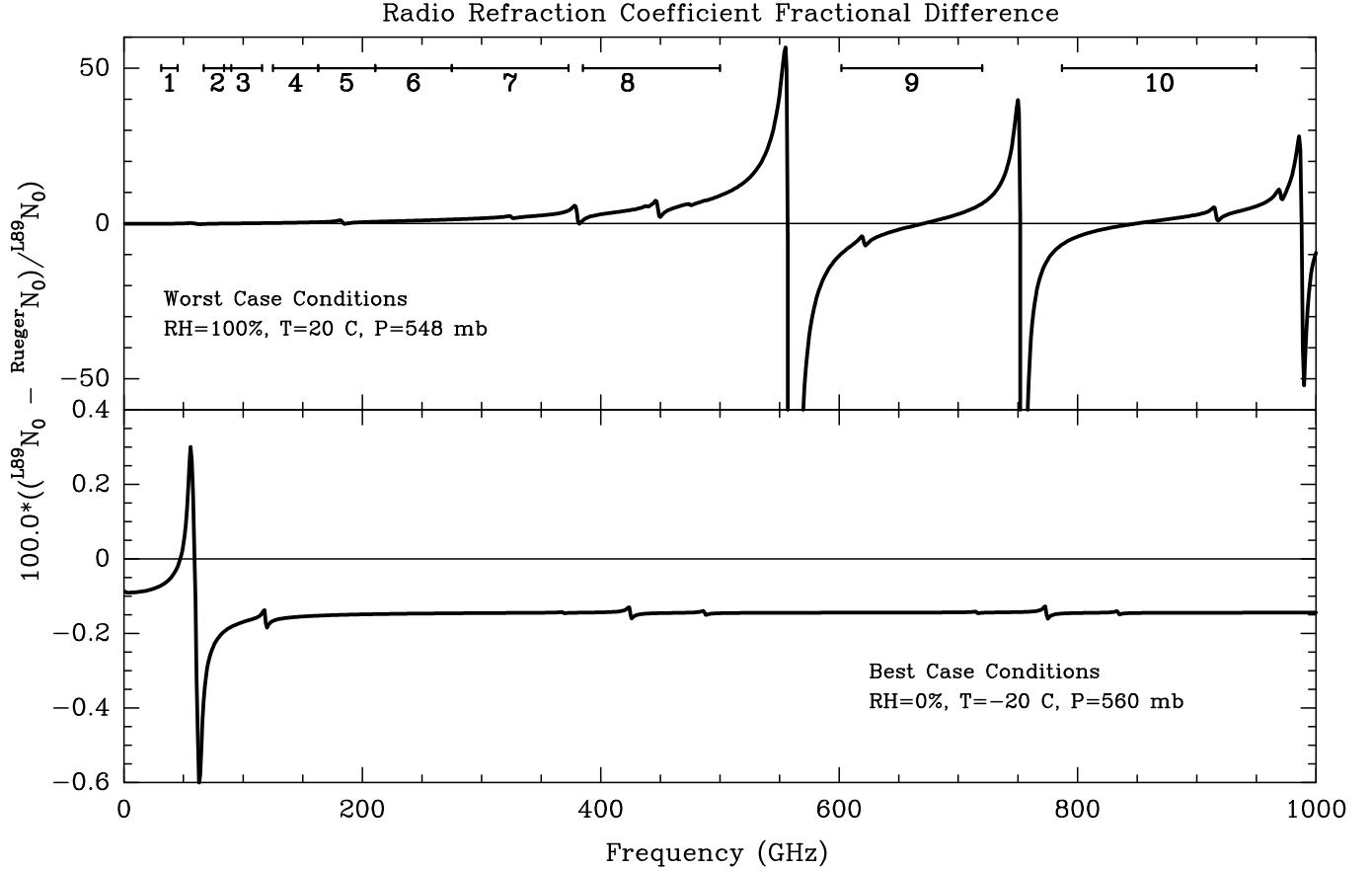


FIG. 4.— Radio refraction coefficient fractional difference between the Rüeger (2002) and Liebe (1989) estimates for N_0^{rad} under the worst (top panel) and best (bottom panel) sets of atmospheric conditions measured at the ALMA site. The best-case condition is equivalent to a troposphere devoid of water vapor. The solid horizontal bars near the top of the diagram show the frequency ranges for the 10 ALMA receiver bands (Wootten & Thompson (2009)).

ric identity for $\tan z$:

$$\begin{aligned} \tan z &= \frac{\sin z}{\sqrt{1 - \sin^2 z}} \\ &= \frac{n_0 r_0 \sin z_0}{\sqrt{n^2 r^2 - n_0^2 r_0^2 \sin^2 z_0}}. \end{aligned} \quad (73)$$

Substituting this expression into our general equation for atmospheric refraction (Equation 22) results in an approximation to the refractive atmospheric bending due to a single-layer Earth atmosphere:

$$R_{spherical} = \int_1^{n_0} \frac{n_0 r_0 \sin z_0}{n(n^2 r^2 - n_0^2 r_0^2 \sin^2 z_0)^{\frac{1}{2}}} dn. \quad (74)$$

As noted in Smart (1962, Chapter III, Section 37), since the height of the Earth's atmosphere at which the refractive medium is located is small in comparison with its radius ($r \ll r_0$), we can use:

$$\frac{r}{r_0} = 1 + \epsilon \quad (75)$$

where $\epsilon \ll 1$ to substitute for $\frac{r}{r_0}$ in Equation 74:

$$\begin{aligned} R_{spherical} &= \int_1^{n_0} \frac{n_0 \sin z_0}{n(n^2 - n_0^2 \sin^2 z)^{\frac{1}{2}}} dn \\ &\quad - \int_1^{n_0} \frac{n_0 \sin z_0 n \epsilon}{(n^2 - n_0^2 \sin^2 z)^{\frac{3}{2}}} dn, \end{aligned} \quad (76)$$

which after integration (See Smart 1962; Green 1985) becomes:

$$R_{spherical} = A \tan z + B \tan^3 z + C \tan^5 z \quad (77)$$

where A, B, and C are constants dependent on the local atmospheric temperature, pressure, and relative humidity. The approximations used to derive Equation 77 are good for $z \leq 75^\circ$. For a plane-parallel single-layer atmosphere all of the terms higher than first order in z are zero, which results in the following equation for the atmospheric refraction (see Equation 10):

$$R_{plane} = A \tan(z). \quad (78)$$

Figure 5 shows some example refraction calculations.

4. REFRACTIVE DELAY DUE TO THE EARTH'S ATMOSPHERE

The calculation of the atmospheric refractive delay parallels that for refractive bending. To illustrate this

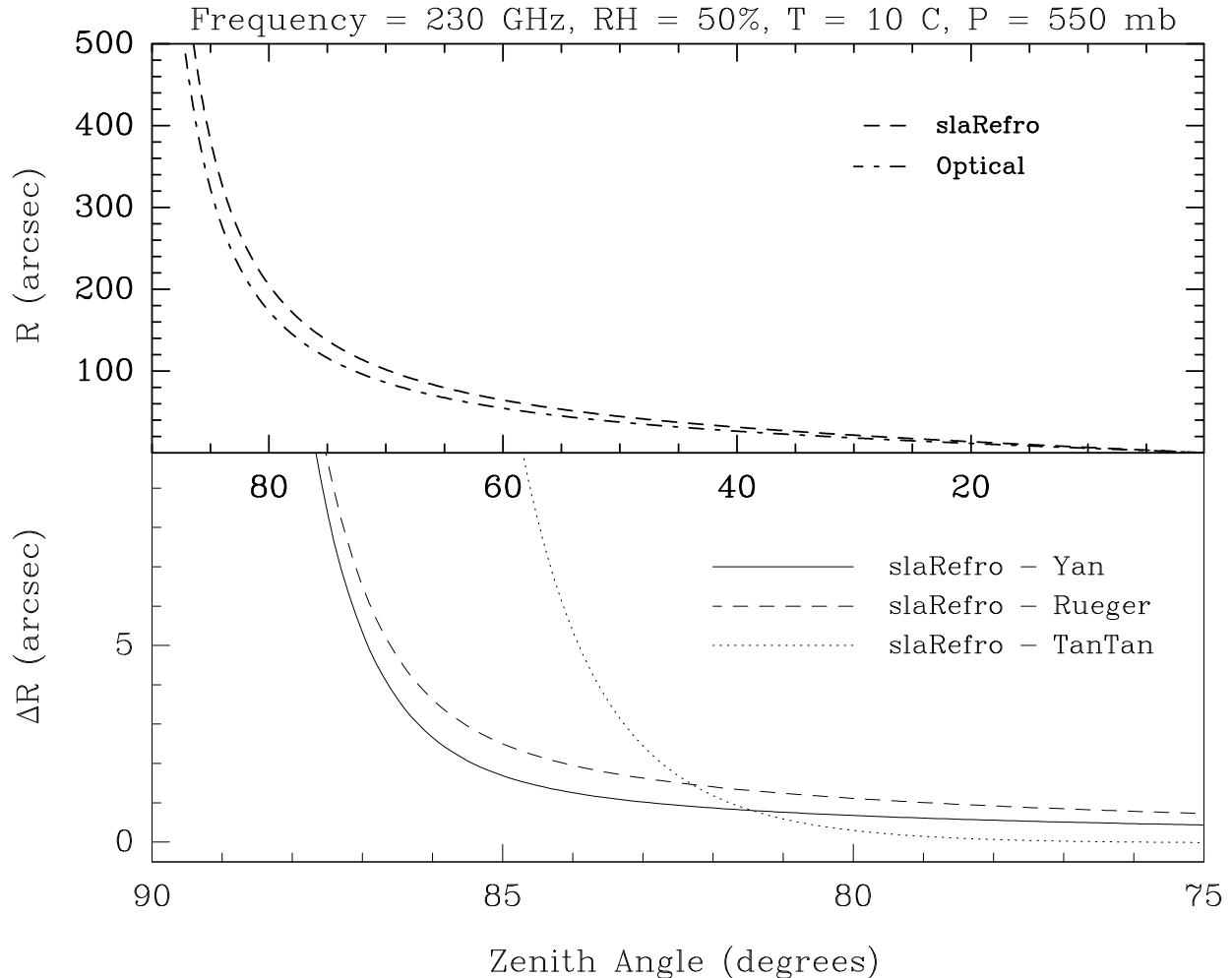


FIG. 5.— Refraction (R ; top) and refraction difference (ΔR ; bottom) as a function of zenith angle for a sampling of refraction models. The refraction function *slaRefro* is a modified version of the Hohenkerk & Sinclair (1985) development of the Auer & Standish (1979) algorithm (Section 3). “Optical” uses Equation A1 with the Yan & Ping (1995) generator function Equation 69. “Rueger” uses Equation 66 with with the Yan & Ping (1995) generator function Equation 69. “TanTan” uses Equation 77 with the coefficient C set to zero and coefficients A and B derived using the *SLALIB* routine *slaRefco*. To derive A and B *slaRefco* forces the refraction Equation 77 to agree with *slaRefro* at $z = 45^\circ$ and $\arctan(4)$, or $\sim 76^\circ$.

fact, the plane-parallel atmosphere approximation to the general equation for atmospheric delay (Equation 4) is given by:

$$\mathcal{L}_{atm} = \int_{r_0}^{\infty} \frac{10^{-6} N(r)}{\cos z} dr \quad (79)$$

In practice the upper limit to the integral in Equation 79 is the top of the stratosphere. By using an atmospheric model to calculate $N(r)$ one can numerically integrate Equation 79 to derive the refractive delay due to the atmosphere. Note that Equation 79 becomes inaccurate at large zenith angles.

To derive a more exact estimate of the atmospheric refractive delay one can assume an atmosphere that is horizontally stratified with an exponential distribution in scale height. Thompson et al. (2001) pp. 516-518 discuss this scenario, the derivation for which we reproduce in

the following. The excess path length is given by:

$$\mathcal{L}_{atm} = 10^{-6} N_0 \int_0^{\infty} \exp\left(-\frac{h}{h_{atm}}\right) dy, \quad (80)$$

where N_0 is the refractivity at the Earth’s surface, h is the height above the Earth’s surface, h_{atm} is the atmospheric scale height, y is the length coordinate along the direction to the source, z is the antenna zenith angle while observing the source, and an exponential distribution to the atmospheric index of refraction has been assumed. One can relate y , h , h_{atm} , and z as follows (see Figure 13-4 in Thompson et al. (2001), page 517) using the cosine rule on the triangle formed by r_0 , y , and $r_0 + h$:

$$(r_0 + h)^2 = r_0^2 + y^2 - 2r_0 y \cos(180^\circ - z). \quad (81)$$

Solving for h yields:

$$h = y \cos z + \frac{y^2 - h^2}{2r_0}. \quad (82)$$

For the nearly right-angled triangle with sides $y \sin(z_i)$, y , and h , we can write:

$$y^2 - h^2 \simeq (y \sin z_i)^2. \quad (83)$$

Since $r_0 \simeq 6370$ km and $h \simeq 12$ km (the typical height of the troposphere, which varies from 9 to 17 km, pole to equator, and seasonally), $r_0 \gg h$. Since $z_i \simeq z + \frac{h}{r_0}$, $z_i \simeq z$ (refractive bending is neglected). The equation for h in terms of y , z , and r_0 then becomes:

$$h \simeq y \cos z + \frac{y^2}{2r_0} \sin^2 z. \quad (84)$$

We can now write the expression for \mathcal{L} as follows:

$$\begin{aligned} \mathcal{L}_{atm} \simeq 10^{-6} N_0 \int_0^\infty \exp\left(-\frac{y}{h_{atm}} \cos z\right) \\ \times \exp\left(-\frac{y^2}{2r_0 h_{atm}} \sin^2 z\right) dy. \end{aligned} \quad (85)$$

Since $\frac{y^2}{r_0 h_{atm}} \ll 1$, the second term in the equation above can be expanded with a Taylor series so that:

$$\begin{aligned} \mathcal{L}_{atm} \simeq 10^{-6} N_0 \int_0^\infty \exp\left(-\frac{y}{h_{atm}} \cos z\right) \\ \times \left(1 - \frac{y^2}{2r_0 h_{atm}} \sin^2 z + \frac{y^4}{8r_0^2 h_{atm}^2} \sin^4 z + \dots\right) dy. \end{aligned} \quad (86)$$

Integration yields:

$$\begin{aligned} \mathcal{L}_{atm} \simeq 10^{-6} N_0 h_{atm} \sec z \\ \times \left(1 - \frac{h_{atm}}{r_0} \tan^2 z + \frac{3h_0^2}{r_0^2} \tan^4 z + \dots\right). \end{aligned} \quad (87)$$

Writing this equation in terms involving $\sec z$, the excess path length \mathcal{L} becomes:

$$\begin{aligned} \mathcal{L}_{atm} \simeq 10^{-6} N_0 h_{atm} \left[\left(1 + \frac{h_{atm}}{r_0} + \frac{3h_0^2}{r_0^2}\right) \sec z \right. \\ \left. - \left(\frac{h_{atm}}{r_0} + \frac{6h_0^2}{r_0^2}\right) \sec^3 z + \frac{3h_0^2}{r_0^2} \sec^5 z + \dots \right]. \end{aligned} \quad (88)$$

Note that one must calculate N_0 using a suitable atmospheric model which uses measurements of the local atmospheric pressure, temperature and relative humidity to derive the resultant differential residual delay. In Figure 6 we show a representative calculation of \mathcal{L}_{atm} for the same set of typical atmospheric conditions on the ALMA site used to characterize the atmospheric refractive bending (R) in Figure 5.

4.1. Differential Excess Atmospheric Delay Between Antennas

In the calculation of the atmospheric delay for the antenna elements in an interferometer, two additional delay corrections need to be considered. The first correction is due to the differential excess path length induced by a non-planar atmosphere (Hinder & Ryle 1971). The second is a correction to N_0 at each antenna which accounts

for differences in the height of the antenna (Az,El) intersection point above the reference point for the local atmospheric parameters for the interferometer.

4.1.1. Differential Atmospheric Curvature Delay Between Antennas

For antenna elements oriented along an east-west baseline observing a source that is transiting, we can estimate the change in excess atmospheric delay between one antenna and another antenna along this baseline. Taking the derivative of \mathcal{L}_{atm} with respect to z and multiplying this derivative by the baseline length D divided by r_0 yields the atmospheric differential delay between two antennas separated by distance D along an east-west baseline:

$$\begin{aligned} \frac{d\mathcal{L}_{atm}}{dz} \simeq \frac{-DN_0 h_0 \tan z}{r_0} \left[\left(1 + \frac{h_0}{r_0} + \frac{3h_0^2}{r_0^2}\right) \sec z \right. \\ \left. - 3 \left(\frac{h_0}{r_0} + \frac{6h_0^2}{r_0^2}\right) \sec^3 z + \frac{15h_0^2}{r_0^2} \sec^5 z + \dots \right] \quad (mm) \end{aligned} \quad (89)$$

where D is in m, h_0 is in km, r_0 is in km, and the result is in mm. Figure 7 shows the results of Equation 89 as a function of N_0 for a range of baseline lengths and source zenith angles. To illustrate the magnitude of this correction to the atmospheric delay, for an antenna separation of ~ 2 km observing a source at a zenith angle of ~ 45 degrees the differential excess atmospheric curvature delay is $\sim 5N_0 \mu\text{m}$. For a typical value of $N_0 \sim 300$ ppm $\frac{d\mathcal{L}_{atm}}{dz} \simeq 1.5$ mm.

4.1.2. Antenna Height Correction to Total Atmospheric Delay

In the calculation of the zenith atmospheric delay at an antenna it is assumed that the atmospheric properties (P, T, RH) are the values measured at the (Az,El) axis intersection point of the antenna. For example, in VLBI each antenna station has a set of associated weather measurements which are used to calculate N_0 . For a clustered array like the VLA or ALMA, the effects of the differences in antenna (Az,El) axis intersection point height above some reference point for the local atmospheric parameters need to be accounted for.

The antenna height correction to the total atmospheric delay can be estimated using a simple atmospheric delay model which corrects for the path difference between each antenna in an array and a reference point at the center of the array. For a clustered array like the VLA, the extra atmospheric path due to a difference in antenna height above the center-of-the-array reference point (ΔH , in ns) is given simply by the change in atmospheric pressure between the antenna array elements. A simple estimate of the magnitude of the antenna height difference correction at the zenith can be obtained by assuming that the pressure P changes linearly with height. Then, for example, 100 cm of additional antenna height out of a total atmospheric height of 8 km would correspond to $\left(\frac{100 \text{ cm}}{8 \text{ km}}\right) P = 0.099 \text{ hPa}$ of pressure differential, where we have assumed that $P = 790 \text{ hPa}$ (typical atmospheric pressure at the VLA site). The change to the dry term of the atmospheric delay is roughly 2.3 mm/hPa. This

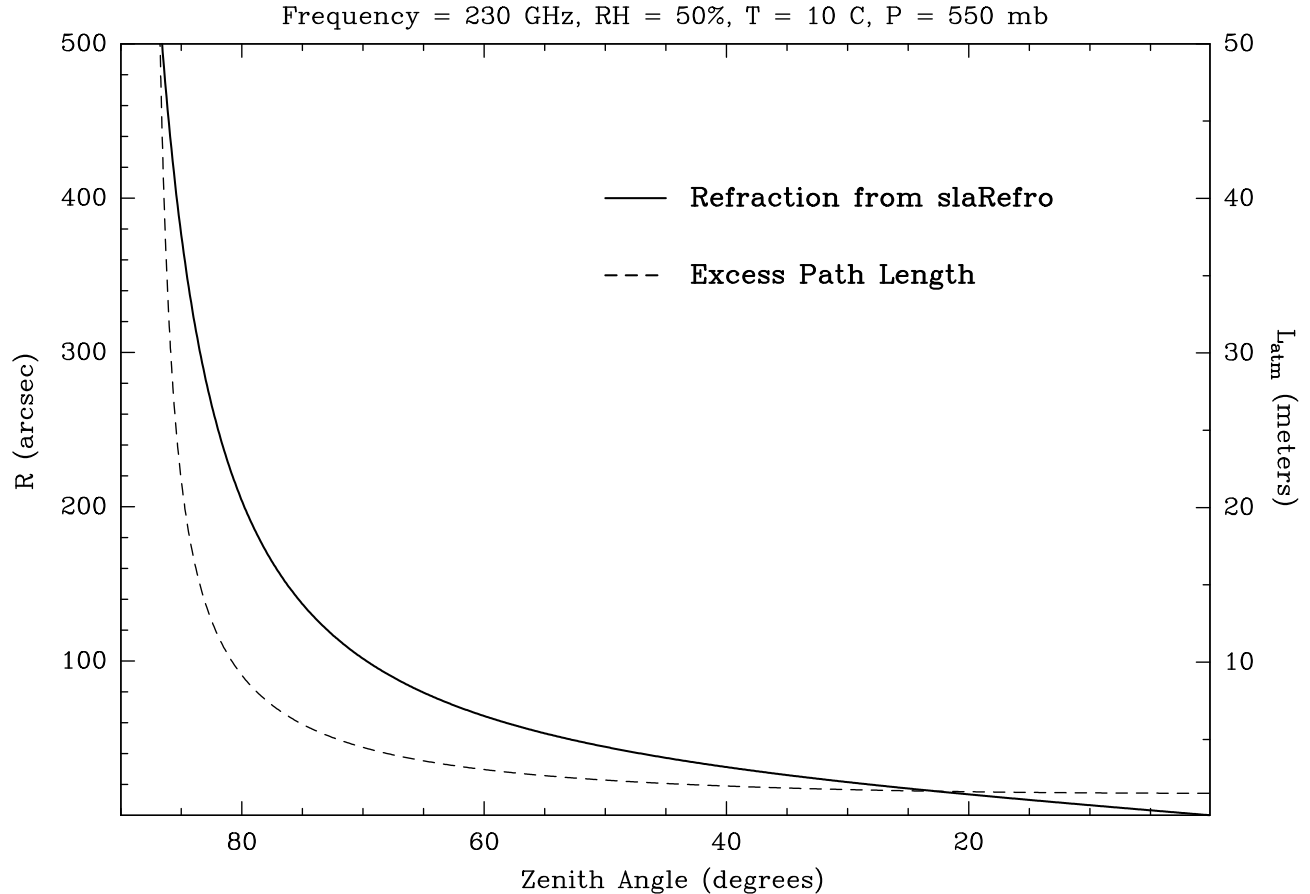


FIG. 6.— Refraction (R ; left) and excess path delay (\mathcal{L}_{atm} ; right) as a function of zenith angle for the atmospheric conditions indicated. The Liebe (1989) atmospheric model has been used to calculate \mathcal{L}_{atm} ($N_0 = 189.416$ ppm).

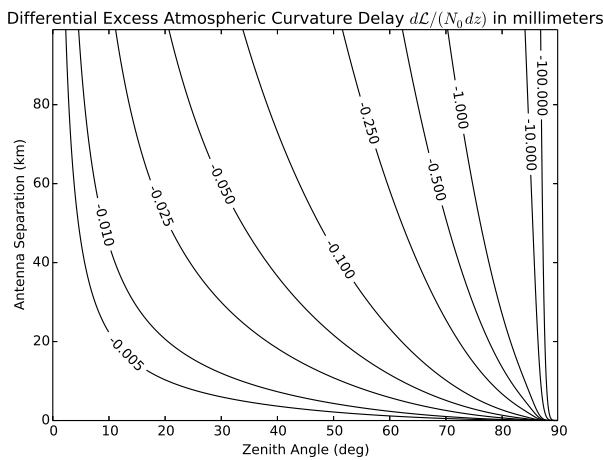


FIG. 7.— Plot of Equation 89 as a function of N_0 for baseline lengths from 10 m to 1 km and zenith angle 1 to 90 degrees.

implies that a pressure change of 0.099 hPa corresponds to approximately 0.228 mm of path difference, which is approximately ten times smaller than the excess delay due to atmospheric curvature (Section 4.1.1).

4.2. Refractive Delay Calculation in Practice

Starting in the 1970's geodesists developed atmospheric refractive delay models which emphasized computational simplicity. As with the derivation of the atmospheric refractive bending, atmospheric refractive delay is generally parameterized as the product of a term which depends upon the local atmospheric parameters (Z) and a term which describes the zenith angle dependence of the atmospheric delay through the use of a “mapping function”⁸ (M).

As was the case for atmospheric refractive bending, in lieu of an atmospheric model based calculation of N it is often convenient to separate the atmospheric delay into contributions due to the dry and wet components of the atmosphere:

$$\mathcal{L}_{atm} = \mathcal{L}_d + \mathcal{L}_w, \quad (90)$$

where \mathcal{L}_d is the contribution due to dry air while \mathcal{L}_w is the contribution due to water vapor. In general \mathcal{L}_d and \mathcal{L}_w are parameterized in terms of a zenith contribution to the delay which is dependent upon local atmospheric conditions (Z) and a mapping function (M) which relate delays at an arbitrary zenith angle z to that at the

⁸ The “mapping function” M used in atmospheric refractive delay calculations is directly analogous to the “generator function” m' sometimes used in the atmospheric refractive bending calculation.

zenith:

$$\begin{aligned}\mathcal{L}_{atm} &= ZM \\ &= Z_d M_d + Z_w M_w\end{aligned}\quad (91)$$

Since z is the unrefracted zenith angle, refractive delay effects are included in the mapping functions M . In the following we describe typical methods for calculating Z and M .

4.2.1. Zenith Delay

The contribution to the atmospheric delay at the zenith (Z) is a measure of the integrated refractivity of the atmosphere at the zenith (N). As was noted in Section 3.1.4 there are closed-form expressions for $N(P, T)$ which are appropriate for calculations at frequencies below 100 GHz. For high-frequency calculations, one must use an atmospheric model.

4.2.2. Mapping Functions

The simplest form for the mapping function (M), which relates the delay at an arbitrary zenith angle z to that at the zenith, is given by the plane-parallel approximation for the Earth's atmosphere:

$$M = \frac{1}{\cos z} \quad (92)$$

This simple form is in practice inadequate, which led Marini (1972) to consider corrections which accounted for the Earth's curvature. Assuming an exponential atmospheric profile where the atmospheric refractivity varies exponentially with height above the antenna, Marini (1972) developed a continued fraction form for the mapping function:

$$M = \frac{1}{\cos z + \frac{a}{\cos z + \frac{b}{\cos z + c}}}, \quad (93)$$

where we include only the first three terms in the continued fraction. The constants a, b, c, d , etc. in the continued fraction forms for the mapping functions presented in this tutorial are generally derived from analytic fits to ray-tracing results of standard atmospheric models. These mapping function constants are often optimized using measurements of the atmospheric distribution of pressure and temperature over an observatory (based on radiosonde measurements, for example). The mapping functions derived in Niell (1996) and Davis et al. (1985) are optimized in this way.

Two slight modifications to the Marini (1972) continued fraction functional form can be implemented to force $M = 1$ at the zenith:

- Normalize Equation 93 as follows:

$$M = \frac{1 + \frac{a}{1 + \frac{b}{1 + c}}}{\cos z + \frac{a}{\cos z + \frac{b}{\cos z + c}}}. \quad (94)$$

See Niell (1996) for a discussion of how to use this form of the mapping function⁹, including derivation of the coefficients a, b , and c .

- Replace the even numbered $\cos z$ terms (i.e. the second, fourth, sixth, etc.) with $\cot z$:

$$M = \frac{1}{\cot z + \frac{a}{\cot z + \frac{b}{\cos z + c}}}. \quad (95)$$

Chao (1974) introduced this modification by truncating the Marini (1972) form to include only two terms.

As noted in Section 3.2, a similar continued-fraction form for the mapping function has been developed by Yan & Ping (1995) and Yan (1996) (Equation 70).

A physically more correct mapping function has been derived by Lanyi (1984). Unlike previous mapping functions, Lanyi's does not fully separate the dry and wet contributions to the delay, which is a more physically correct approximation. It is based on an ideal model atmosphere whose temperature is constant from the surface to the inversion layer h_1 , then decreases linearly with height at rate W from h_1 to the tropopause height h_2 , then is assumed to be constant above h_2 . This mapping function is designed to be a semi-analytic approximation to the atmospheric delay integral that retains an explicit temperature profile that can be determined using meteorological measurements. The mapping function is expanded as a second-order polynomial in Z_d and Z_w , plus the largest third-order term. It is nonlinear in Z_d and Z_w . It also contains terms which couple Z_d and Z_w , thus including terms which arise from the bending of the electromagnetic wave path through the atmosphere. The functional form for the atmospheric delay in this Lanyi (1984) model is given by:

$$\mathcal{L}_{atm} = \frac{F(E)}{\sin E}, \quad (96)$$

where

$$\begin{aligned}F(E) &= F_d(E)Z_d + F_w(E)Z_w \\ &+ \frac{F_{b1}(E)Z_d^2 + 2F_{b2}(E)Z_dZ_w + F_{b3}(E)Z_w^2 + F_{b4}(E)Z_d^3}{\Delta} + \frac{F_{b4}(E)Z_d^3}{\Delta^2},\end{aligned}\quad (97)$$

where Z_d = dry atmospheric zenith delay, Z_w = wet atmospheric zenith delay, F_{bn} = n -th bending contributions to the delay, Δ = dry atmospheric scale height = $\frac{kT_0}{mg_m}$, k = Boltzmann's constant, T_0 = daily average surface temperature, m = mean molecular mass of dry air, and g_m = gravitational acceleration of the center of gravity of the air column. Standard values of k , m , $T_0 = 292K$ (appropriate for mid-latitudes), $g_m = 978.37 \text{ cm/s}^2$, and $\Delta = 8.6 \text{ km}$, are assumed. The dry, wet, and bending contributions are expressed in terms of moments of the refractivity. The bending terms are evaluated for the

⁹ Note that Equation 4 in Niell (1996) contains a typo. The numerator should be just A , rather than $\frac{1}{A}$. See Niell (2001). Equation 94 lists the correct form for this equation.

ideal model atmosphere and thus give the dependence of the delay on the four parameters T_0 , W , h_1 , and h_2 . Therefore, the Lanyi (1984) model relies upon accurate surface meteorological measurements at the time of the observations to which the delay model is applied.

Note that, contrary to the rest of this tutorial, we have cast the functional form for the Lanyi (1984) atmospheric delay in terms of the elevation (E), which is the coordinate used by Lanyi (1984), rather than zenith angle. As the terms in Equation 97 are complex functions of E , we opted not to provide a version of Equation 97 which used z as the dependent variable, mainly out of fear of possibly adding errors to this discussion.

4.2.3. Mapping Function Summary

Differences between the various mapping functions increase rapidly at high zenith angle ($z > 80^\circ$). Lanyi (1984) has compared the (Marini 1972, Equation 93), (Chao 1974, Equation 95), and (Lanyi 1984, Equation 96) mapping functions for atmospheric refractive delay measurements at radio wavelengths. For $z < 50^\circ$ these mapping functions differ by less than 4 mm in excess path length. At high zenith angles ($z > 80^\circ$), though, these differences increase to 60 mm, rapidly increasing for even higher zenith angles.

Errors in the atmospheric path delay to an antenna are equivalent to errors in the vertical position of the antenna. Furthermore, for an interferometric antenna array errors in the vertical position of an antenna are to first-order proportional to an error in the interferometric baseline involving that antenna. Interferometric array baseline determination relies on measurements of astronomical point sources observed over as large a range in zenith angle as possible. Davis et al. (1985) showed that limiting the maximum zenith angle in a baseline measurement from 85 to 80 degrees results in an error in the baseline determination of $\sim 10^{-5}$. As baselines in an interferometric array must be measured to an accuracy of better than one part in 10^7 (Thompson et al. 2001) so as not to degrade the sensitivity of the measurements made with the interferometric array, errors in the determination of the atmospheric refractive delay can be significant for Very Long Baseline Interferometric (VLBI) measurements and/or interferometric measurements at millimeter and submillimeter wavelengths.

5. SOME BACKGROUND ON GENERATOR FUNCTION REFERENCES

In the following we give some background information on some of the references quoted in this section:

Niell (1996):: *Global Mapping Functions for the Atmospheric Delay at Radio Wavelengths*. The standard reference for the derivation of a global mapping function for atmospheric delay. This derivation of the mapping function is noteworthy in that it attempts to represent analytically the global weather variations as a function of location (latitude) and time of year, and contains no adjustable parameters (i.e. does not require input pressure and temperature for each station). Note that Equation 4 in Niell (1996) has a typo whereby the terms which are printed as “1/term” in both the numerator and denominator should really be just “term” in both the numerator and denominator.

Davis et al. (1985):: *Geodesy by Radio Interferometry: Effects of Atmospheric Modeling Errors on Estimates of Baseline Length*. An application of a modified Smith-Weintraub refractivity and the Niell mapping functions.

Sovers et al. (1998):: *Astrometry and Geodesy with Radio Interferometry: Experiments, Models, Results*. An excellent overview paper describing the details involved in calculating geometric and atmospheric delay. Uses the Lanyi (1984) model for the mapping function, which is a significant departure from the standard (i.e. Niell (1996)) mapping functions which derive from the Marini (1972) reduced fraction functional form.

Lanyi (1984):: *Tropospheric Delay Effects in Radio Interferometry*. Derivation of a new “tropospheric” (really atmospheric) mapping function which, unlike previous mapping functions, takes account of second and third order effects in the refractivity which are due to refractive bending. This derivation of the mapping function is noteworthy in that it does not fully separate the dry and wet contributions to the delay, making it a physically more exact representation. It is claimed to be more accurate than previous (i.e. Niell) mapping functions for $z < 86^\circ$, and the error due to the derived analytic form for the mapping function is estimated to be less than 0.02% for $z < 84^\circ$.

Yan & Ping (1995):: *The Generator Function Method of the Tropospheric Refraction Corrections*. Another derivation of a new “tropospheric” (really atmospheric) mapping function. A cousin to existing reduced-fraction expansions of the mapping function.

Yan (1996):: *A New Expression for Astronomical Refraction*. Related to the Yan & Ping (1995) reference above, but applied to the refraction calculation problem. Using the Yan & Ping (1995) and Yan (1996) references one can apply a unified formalism to both the atmosphere-induced refractive delay and bending problems.

6. CONCLUSIONS

Modern astronomical measurements often require sub-arcsecond position accuracy. For the simplified model atmospheres presented in this tutorial, which assume a spherical structure with hydrostatic equilibrium for the dry component (mainly the stratosphere) and uniform mixing of the wet component (mainly the troposphere) of the Earth’s atmosphere, radio astronomical measurements with position accuracy $\lesssim 1''$ at zenith angles $\lesssim 75^\circ$ are achievable. Any of the functional forms for refractive bending and delay which assume a spherical atmosphere are satisfactory in this simplified scenario. For measurements at zenith angles $\gtrsim 75^\circ$, or for more realistic atmospheric conditions which violate the simple scenario described above, or when higher positional accuracy than $\sim 1''$ is required, more care needs to be taken in the algorithm choice for atmospheric refractive bending and delay.

For accurate calculation of the refractive electromagnetic wave bending and propagation delay at an Earth-bound observatory, we recommend the following:

1. *Refractive Bending Calculation:* Use the Auer & Standish (2000) method (Equation 29) with the procedure described in Section 3. The refractivity ($N(P, T)$) is derived from an atmospheric model such as Liebe (1989) or Pardo et al. (2001).
2. *Refractive Delay Calculation:* Use Equation 79 with refractivity derived from an atmospheric model. The best of the mapping function solu-

tions to \mathcal{L}_{atm} is the Lanyi (1984) algorithm (Equation 96), which appears to be quite accurate to zenith angles as high as $\sim 85^\circ$.

JGM benefited greatly from discussions regarding the proper calculation of atmospheric path delay with Darrel Emerson, Dick Thompson, and Ed Fomalont. The referee for this manuscript, Jim Moran, provided invaluable advice which resulted in a greatly improved manuscript. The National Radio Astronomy Observatory is a facility of the National Science Foundation operated under cooperative agreement by Associated Universities, Inc.

APPENDIX

ATMOSPHERIC OPTICAL REFRACTIVITY

Refractivity in the optical is cast in a slightly different form than that in the radio due to the fact that at optical wavelengths dispersion is important, and color must always be taken into account. Birch & Downs (1993) (see also Livengood et al. (1999)) state that the optical refractivity is given by the following:

$$N_0^{opt} = N_{STP} \times N_{TP} - N_{RH} \quad (\text{A1})$$

where

$$N_{STP} = 83.4305 + \frac{24062.94}{130 - \lambda^{-2}} + \frac{159.99}{38.9 - \lambda^{-2}} \quad (\text{A2})$$

$$N_{TP} = \frac{P_d}{1.01325 \times 10^3} \frac{(273.15 + 15)}{T} \frac{[1 + (3.25602 - 0.00972T)P_d \times 10^{-6}]}{1.00047} \quad (\text{A3})$$

$$N_{RH} = P_w \times (37.345 - 0.401\lambda^{-2}) \times 10^{-3} \quad (\text{A4})$$

with P_d and P_w in hPa, T in K, and λ in μm . Note that we have ignored the small correction for an increase in CO_2 concentration in Equation A1.

ACCELERATION DUE TO GRAVITY

The mean acceleration due to gravity (g_m) at the center of mass of a vertical column of air above an observer is given by:

$$g_m = \frac{\int_0^\infty dx \rho(x) g(x)}{\int_0^\infty dx \rho(x)}. \quad (\text{B1})$$

By expanding $g(x)$ to first-order in x , fits to harmonic forms of g_m as a function of latitude (ϕ) can be derived. Geodesists use a closed form of this harmonic function fit, known as the Somigliana-Pizzetti formula (Pizzetti 1894; Somigliana 1929; Moritz 1980):

$$\begin{aligned} g_m &= \frac{a\gamma_e \cos^2 \phi + b\gamma_p \sin^2 \phi}{\sqrt{a^2 \cos^2 \phi + b^2 \sin^2 \phi}} \\ &= \gamma_e \frac{1 + \kappa \sin^2 \phi}{\sqrt{1 + e^2 \sin^2 \phi}}, \end{aligned} \quad (\text{B2})$$

where a and b are the semimajor and semiminor axes of the geocentric gravitational potential ellipsoid of revolution chosen to define the Earth's gravitational potential, γ_e and γ_p are the theoretical gravitational acceleration at the Earth's equator and pole, respectively, and e , the first eccentricity of the ellipsoid, and κ are defined as follows:

$$e \equiv \sqrt{1 - \left(\frac{b}{a}\right)^2} \quad (\text{B3})$$

$$\kappa \equiv \frac{b\gamma_p}{a\gamma_e} - 1. \quad (\text{B4})$$

Two Chebyshev approximations to Equation B2 are in common usage in geophysics. The first has a relative accuracy of $10^{-3} \mu\text{m sec}^{-2}$ (Moritz 1980) and is given by:

$$g_m = \gamma_e (1 + \alpha_0 \sin^2 \phi + \alpha_1 \sin^4 \phi + \alpha_2 \sin^6 \phi + \alpha_3 \sin^8 \phi), \quad (\text{B5})$$

while the second has a relative accuracy of $1 \mu\text{m sec}^{-2}$ (Moritz 1980) and is given by:

$$g_m = \gamma_e (\beta_0 \sin^2 \phi + \beta_1 \sin^2 2\phi). \quad (\text{B6})$$

Equation B6 is the approximation most often used to compute the latitudinal dependence of gravitational acceleration in geophysics.

Most derivations of the mean acceleration due to gravity at a given latitude calculate this quantity with reference to the center of mass of a vertical column of air above an observer (H_c). It is often convenient to calculate g_m as a function of the height of an observer above sea level on the surface of the Earth (h_0). Saastamoinen (1972) points out that, due to the poleward slope of the tropopause and seasonal variations of T and P , regional and seasonal variations in H_c tend to be smoothed out. To an accuracy of ± 0.4 km, H_c and h_0 are related by:

$$H_c = 0.9 h_0 + 7.3 \text{ km} \quad (\text{B7})$$

In the following we list a variety of formulations for g_m as functions of latitude (ϕ) and observer height above sea level (h_0 , in km). These expressions for g_m differ by the assumed gravitational potential ellipsoid and, with the exception of Equation B8, rely on the use of the approximate form for g_m given in Equation B6. For observer height above sea level ranging from 0 to 25 m all of the expressions for g_m listed in this appendix differ by less than 0.015%. Any of the g_m listed below are sufficient for the refraction application. Note also that none of these expressions for g_m take account of local gravitational variations such as from nearby mountains, which can be significant.

The expression for g_m that we have adopted in this work comes from the definition adopted by the World Geodetic System 1984 (WGS84), with an additional height correction:

$$\begin{aligned} g_m^{WGS84} &= 9.7803267714 \left(\frac{1 + 0.00193185138639 \sin^2 \phi}{\sqrt{1 - 0.00669437999013 \sin^2 \phi}} \right) - 0.003086 H_c \text{ m/s}^2 \\ &= 9.7803267714 \left(\frac{1 + 0.00193185138639 \sin^2 \phi}{\sqrt{1 - 0.00669437999013 \sin^2 \phi}} \right) - 0.02253 \\ &\quad - 0.0027774 h_0 \text{ m/s}^2 \end{aligned} \quad (\text{B8})$$

where h_0 is the height of the observer and H_c is the height of the center of mass of the vertical column of air above the observer, both in km. Figure 8 shows how g_m^{WGS84} varies as a function of latitude and observer height above sea level.

Allen (1973) quotes the following form:

$$\begin{aligned} g_m^{Allen} &= 9.80612 - 0.025865 \cos(2\phi) + 0.000058 \cos^2(2\phi) - 0.00308 H_c \text{ m/s}^2 \\ &= 9.780313 (1 + 0.005289 \sin^2 \phi - 0.0000059 \sin^2(2\phi) - 0.000315 H_c) \text{ m/s}^2 \\ &= 9.757823 (1 + 0.005301 \sin^2 \phi - 0.0000059 \sin^2(2\phi) - 0.000284 h_0) \text{ m/s}^2 \end{aligned} \quad (\text{B9})$$

From Urban & Seidelmann (2013) (which is also the form used in *SLALIB* and by Hohenkerk & Sinclair (1985), and where h_0 is in km):

$$g_m^{ES} = 9.784 (1.0 - 0.0026 \cos(2\phi) - 0.00028 h_0) \text{ m/s}^2 \quad (\text{B10})$$

The CRC handbook gives yet another variant:

$$\begin{aligned} g_m^{CRC} &= 9.780356 (1 + 0.0052885 \sin^2 \phi - 0.0000059 \sin^2(2\phi)) - 0.003086 H_c \text{ m/s}^2 \\ &= 9.757828 (1 + 0.005301 \sin^2 \phi - 0.0000059 \sin^2(2\phi) - 0.000284 h_0) \text{ m/s}^2 \end{aligned} \quad (\text{B11})$$

with the reference Jursa (1985). The web site

http://geophysics.ou.edu/solid_earth/notes/potential/igf.htm

lists the following, which is based on the Geodetic Reference System 1967:

$$\begin{aligned} g_m^{IGF67} &= 9.78031846 (1 + 0.0053024 \sin^2 \phi - 0.0000058 \sin^2(2\phi)) - 0.003086 H_c \text{ m/s}^2 \\ &= 9.757791 (1 + 0.005315 \sin^2 \phi - 0.0000058 \sin^2(2\phi) - 0.000284 h_0) \text{ m/s}^2 \end{aligned} \quad (\text{B12})$$

where we have added the free-air and height correction term. Finally, Saastamoinen (1972) derives:

$$\begin{aligned} g_m^{Saast} &= 9.8062 (1 - 0.00265 \cos(2\phi) - 0.00031 H_c) \\ &= 9.784 (1 - 0.00266 \cos(2\phi) - 0.00028 h_0) \end{aligned} \quad (\text{B13})$$

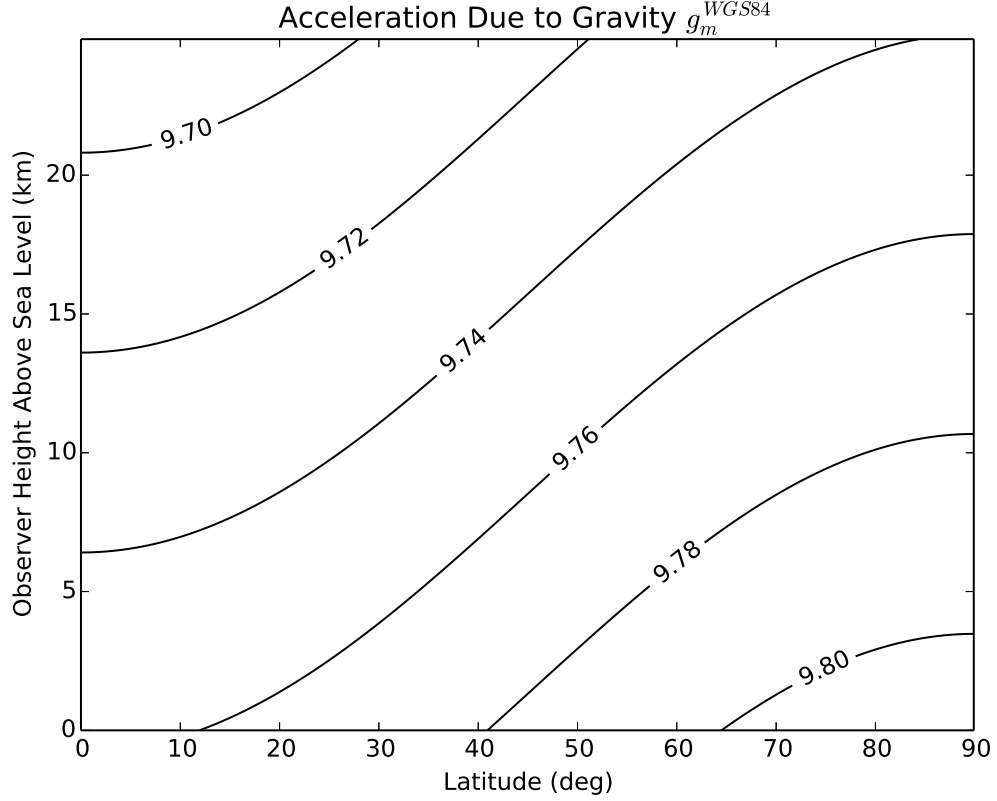


FIG. 8.— Acceleration due to gravity g_m^{WGSS4} as a function of observer latitude and height above sea level.

RELATIVE HUMIDITY AND SATURATION VAPOR PRESSURE

Note that the relative humidity at the observer (RH_0 , in percent) is related to the saturation vapor pressure (e_{sat} , in hPa; Buck (1981)) as follows (see Crane (1976))

$$e_{sat} = (1.0007 + 3.46 \times 10^{-6} P_0) 6.1121 \exp \left[\frac{17.502 T_0}{T_0 + 240.97} \right] \quad (C1)$$

$$P_{w0} = e_{sat} RH_0 \left[1 - (1 - RH_0) \frac{e_{sat}}{P_0} \right]^{-1} \quad (C2)$$

This relationship between e_{sat} , P_{w0} , and RH_0 is useful when using expressions for N_0 which involve linear and quadratic expansions in P_0 and P_{w0} . Unfortunately, this complicated form for e_{sat} does not yield itself to closed-form integration.

By assuming that the relative humidity remains constant throughout the troposphere, and equal to its value at the observer ($RH(r) = RH_0$), we can write:

$$\frac{P_w}{P_{w0}} = \frac{e_{sat}(P, T)}{e_{sat}(P_0, T_0)} \quad (C3)$$

Tabulated values of e_{sat} versus T indicate that:

$$\frac{e_{sat}(P, T)}{e_{sat}(P_0, T_0)} = \left(\frac{T}{T_0} \right)^\gamma \quad (C4)$$

which yields:

$$\frac{P_w}{P_{w0}} = \left(\frac{T}{T_0} \right)^\gamma \quad (C5)$$

As noted by Sinclair (1982) and Hohenkerk & Sinclair (1985), the power index γ is derived by fitting to the tabulated values of P_{sat} versus T given in List (1952). This fit produces the following:

$$P_{sat} = \left(\frac{T}{247.1} \right)^{18.36} \quad (C6)$$

Comparing this expression with that derived by Buck (1981) (Equation C1) for P between 600 hPa and 1200 hPa and T between -30 C and $+20\text{ C}$ indicates agreement to within $\pm 0.2\text{ hPa}$. Therefore, the approximate relation between P_{sat} and T (Equation C6) represents a good approximation over this relevant range of P and T .

REFERENCES

- Allen, C. W. 1973, *Astrophysical quantities* (London: Athlone Press (2nd edition), 1964)
- Auer, L. H., & Standish, E. M. 1979, *Astronomical Refraction: Computational Method for All Zenith Angles*, Tech. rep., Yale University Astronomy Department
- . 2000, *AJ*, 119, 2472
- Bean, B. R., & Dutton, E. J. 1966, *Radio Meteorology* (U.S. Department of Commerce, National Bureau of Standards)
- Birch, K. P., & Downs, M. J. 1993, *Metrologia*, 30, 155
- Brussaard, G., & Watson, P. A. 1995, *Atmospheric Modelling and Millimeter Wave Propagation* (London; New York: Chapman & Hall, 1995), 254
- Buck, A. L. 1981, *J. Appl. Meteor.*, 20, 1527
- Chao, C. C. 1974, *The Tropospheric Calibration Model for Mariner Mars 1971*, Tech. Rep. 32-1587, Jet Propulsion Laboratory
- Condon, J. J. 2004, *Refraction Corrections for the GBT*, Tech. Rep. PTCs Project Note 35.2, National Radio Astronomy Observatory
- Crane, R. K. 1976, *Methods of Experimental Physics, Part C: Radio Observations* (New York; San Francisco; London: Academic Press, 1976), 188
- Davis, J. L., Herring, T. A., Shapiro, I. I., Rogers, A. E. E., & Elgered, G. 1985, *Radio Science*, 20, 1593
- Garfinkel, B. 1944, *AJ*, 50, 169
- . 1967, *AJ*, 72, 235
- Green, R. M. 1985, *Spherical Astronomy*. (Cambridge [Cambridgeshire] University Press, 1985)
- Hinder, R., & Ryle, M. 1971, *MNRAS*, 154, 229
- Hohenkerk, C. Y., & Sinclair, A. T. 1985, *The Computation of Angular Atmospheric Refraction at Large Zenith Angles*, Tech. Rep. 63, HM Nautical Almanac Office
- Jursa, A. S. 1985, *Handbook of geophysics and the space environment*, 4th edition, Tech. rep., United States Air Force
- Lanyi, G. E. 1984, *Telecommunications and Data Acquisition Progress Report*, 78, 152
- Liebe, H., & Hopponen, J. 1977, *IEEE Trans. Antennas and Propagation*, 25, 336
- Liebe, H. J. 1989, *International Journal of Infrared and Millimeter Waves*, 10, 631
- Liebe, H. J., Hufford, G. A., & Cotton, M. G. 1993, *Propagation Modeling of Moist Air and Suspended Water/Ice Particles at Frequencies Below 1000 GHz*, Tech. rep., Advisory Group for Aerospace Research & Development
- List, R. J. 1952, *Quarterly Journal of the Royal Meteorological Society*, 78, 288
- Livengood, T. A., Fast, K. E., Kostiuk, T., et al. 1999, *PASP*, 111, 512
- Mangum, J. G. 2001, *A Telescope Pointing Algorithm for ALMA*, Tech. Rep. Memo 366, National Radio Astronomy Observatory
- Marini, J. W. 1972, *Radio Science*, 7, 223
- Moritz, H. 1980, *Bulletin Geodesique*, 54, 395
- Murray, C. A. 1983, *Vectorial Astrometry* (Bristol: Adam Hilger Ltd., 1983)
- Niell, A. E. 1996, *Journal of Geophysical Research: Solid Earth*, 101, 3227
- . 2001, *Physics and Chemistry of the Earth, Part A: Solid Earth and Geodesy*, 26, 475, proceedings of the First COST Action 716 Workshop Towards Operational GPS Meteorology and the Second Network Workshop of the International GPS Service (IGS)
- Pardo, J. R., Cernicharo, J., & Serabyn, E. 2001, *Antennas and Propagation, IEEE Transactions on*, 49, 1683
- Pizzetti, P. 1894, *Atti Reale Accademia dei Lincei*, 3, 166
- Rüeger, J. M. 2002, *Refractive Index Formulae for Electronic Distance Measurement with Radio and Millimetre Waves*, Tech. Rep. UNISURV S-68, 2002, School of Surveying and Spatial Information Systems, University of New South Wales, UNSW, Sydney, NSW 2052, Australia
- Saastamoinen, J. 1972, *Geophysics Monogram Series*, 15, 247
- Sinclair, A. T. 1982, *The Effect of Atmospheric Refraction on Laser Ranging Data*, Tech. Rep. 59, HM Nautical Almanac Office
- Smart, W. M. 1962, *Text-Book on Spherical Astronomy* (Cambridge [Eng.] University Press, 1962. [5th ed.]
- Smith, E. K., & Weintraub, S. 1953, *Proceedings of the IRE*, 41, 1035
- Somigliana, C. 1929, *Mem. Soc. Astron. Italiana*, 4, 425
- Sovers, O. J., Fanselow, J. L., & Jacobs, C. S. 1998, *Rev. Mod. Phys.*, 70, 1393
- Thompson, A. R., Moran, J. M., & Swenson, Jr., G. W. 2001, *Interferometry and Synthesis in Radio Astronomy*, 2nd Edition (New York : Wiley, 2001)
- Urban, S., & Seidelmann, P. K. 2013, *Explanatory Supplement to the Astronomical Almanac* (University Science Books)
- Wootten, A., & Thompson, A. R. 2009, *IEEE Proceedings*, 97, 1463
- Yan, H. 1996, *AJ*, 112, 1312
- Yan, H., & Ping, J. 1995, *AJ*, 110, 934
- Young, A. T. 2000, in *Bulletin of the American Astronomical Society*, Vol. 197, American Astronomical Society Meeting Abstracts, 101
- Young, A. T. 2004, *AJ*, 127, 3622